energies

MDPI

Article

Effects of Water Leaching on the Ash Sintering Problems of Wheat Straw

Shibo Wu, Jiannan Chen *, Daoping Peng *, Zheng Wu, Qin Li and Tao Huang

Faculty of Geosciences and Environmental Engineering, Southwest Jiaotong University, Chengdu 611756, China; shibowu1001@outlook.com (S.W.); wowzzz0017@163.com (Z.W.); liqin0623@outlook.com (Q.L.); taohuang70@126.com (T.H.)

* Correspondence: jchen@swjtu.edu.cn (J.C.); pdp0330@swjtu.edu.cn (D.P.); Tel.: +86-28-8760-2673 (J.C.); +86-13438284493 (D.P.)

Received: 7 December 2018; Accepted: 23 January 2019; Published: 26 January 2019

Abstract: Biomass energy has been used for decades in lieu of fossil fuels. However, biomass, such as wheat straw, typically contains a high concentration of alkali elements, which is likely to induce unfavorable conditions during combustion, such as slagging, agglomeration, and corrosion in the boiler. This study investigated the effects of leaching on the chemical compounds and sintering temperatures of wheat straw ash before and after leaching by tap water. Ash melting and sintering degree tests were conducted using hot-stage microscopy and a scanning electron microscope, respectively. The results show that the ash content in wheat straw decreased by 26.09% (from 4.14% to 3.06%) following leaching, as did the chlorine (Cl), sulfur (S), and nitrogen (N). Meanwhile, the ash-related elements such as potassium (K), magnesium (Mg), and silicon (Si) reduced after leaching too. Additionally, the higher heating value increased slightly, from 19.25 to 19.53 MJ/kg. At the same time, leaching improved the ash melting temperatures of wheat straw during combustion and minimized the ash sintering degree. Similar results were also shown in scanning electron microscope (SEM) images, which clearly indicated that the leached samples had a lighter sintering degree than the original samples. Overall, the leaching process had a positive effect on the ash sintering problems of wheat straw.

Keywords: leaching process; wheat straw; sintering temperature; scanning electron microscope

1. Introduction

Human activities demand a vast amount of energy. Fossil fuel has been the most prevalent energy source for the past several decades. However, population growth and economic development have greatly stimulated an increase in overall energy consumption, which, in turn, has accelerated the use of fossil fuels. The yearly energy demand throughout the world doubled between 2000 and 1970, and, in addition, it increased by 26% from 2000 to 2010 [1]. Because of the rapid depletion of fossil fuels, many people are now facing an energy crisis and its byproducts, such as energy contention, financial crises, regional conflicts, etc. The consumption of fossil fuels also emits greenhouse gases (GHGs), inducing environmental issues such as acid rain, haze pollution, and global warming. GHG emission has alarmingly increased during the past 50 years, resulting in global warming. The emission of carbon dioxide has increased by 100%, while the emission of other GHGs (such as methane and nitrous oxide) has increased by 30% during the past 50 years [2].

Currently, there is a growing interest in utilizing biomass residues for energy purposes in lieu of fossil fuels [3–10]. As a potential energy resource, biomass could provide solutions for economic, political, and environmental problems, such as fossil fuel dependence, job opportunities per unit of energy produced, and adverse environmental impact. Additionally, biomass residues

are readily available and renewable for potential energy sources. Currently, cereal residues are considered among the most important biomass energy resources because of their vast production [4]. During 2013, cereal crops such as wheat and rice provided more than 670 million metric tons of food, dominating human food supplies [5].

Challenges in both the fuel preparation and burning processes of cereal residues, such as gathering, carriage, pre-treatment, pelleting, and combusting, have attracted the attention of scholars and industries, particularly ash-related problems such as ash sintering, agglomeration, and corrosion induced while burning in boilers [6,9–16]. High concentrations of Cl combined with alkali metals, such as Na and K, in biomass fuels typically generate sediments during the combustion process. The sediments, such as sinters on the super heater, agglomerate on the water wall, and corrosion of the tube surface occurs not only in fluidized boilers, but also in grate furnaces, and has obvious negative effects on boiler efficiency [10–13,15].

Various measures, such as water or acidic leaching, mineral addition, and co-firing with fossil fuels, have been adopted to solve the aforementioned biomass ash-related problems by optimizing the fuel chemical compositions with low vaporized alkaline compounds [15]. Water or acidic washing (or leaching) directly removes water-soluble elements (e.g., K, Ca, Na, and Cl) from the biomass, which improves biomass fuel characteristics at high temperatures and reduces ash deposits during combustion [17–24]. The heating value in most biomass utilization can be enhanced by the removal of water-soluble inorganic compounds, while no significant loss of organics has been observed [18]. Additionally, acidic pollutants and toxic species can be effectively reduced during the washing process before biomass combustion [17,18].

Currently, the most prevalent leaching techniques are post-harvest and natural precipitation techniques. Liaw et al. [19] analyzed the differences of leaching characteristics between batch and semi-continuous operation; meanwhile, Yu et al. [20] investigated the effects of both the biomass to water ratio and leaching time during the washing process. Moreover, Bakker et al. [22] studied the practical application of natural leaching for improving the thermal conversion of rice straw. Both techniques could effectively remove large quantities of alkaline compounds (e.g., Cl, S, and K) or ash content.

The existing studies mainly focus on the ash sintering temperature removal of chemical compounds by leaching [17,25,26]. However, the microstructure of ash before or after leaching under furnace temperatures, that is, the direct inspection of sedimentation or agglomeration, is yet to be understood. The microstructure of biomass ash under combustion shows clear sintering degrees, considering the loose degree and ash structure. Additionally, the sintered surfaces of ash particles can be captured by microscopic observation. Wang et al. [27] adopted scanning electron microscopy—energy dispersive X-ray spectrometry (SEM-EDX)—to investigate the effects of additives on ash sintering characteristics, and found that the melting of rye straw ash could be attributed to the formation of potassium silicates with a low melting temperature and phosphates with a high K/Ca ratio. Moreover, microstructural observation of the ash particle formation process of rice straw burnt in a fluidized bed combustor was investigated by Liu et al. [13].

This study evaluates the effect of leaching on the chemical compounds and sintering temperature of ash, as well as ash sintering degrees, using tap water. Tap water was used because it is simple, economical (€2.07 /m^3 of tap water, rather than €100 /m^3 of distilled water), readily available, and feasible. The microstructure of the ash from wheat straw were examined using a SEM to examine the process of agglomeration and sedimentation of wheat straw heated at selected temperatures (hierarchically simulated boiler temperatures, from 700 to 1000 °C) before and after leaching. Furthermore, a discussion of the partial correlation between ash-related elements and the shrinkage start temperature is also provided.

2. Materials and Methods

2.1. Sampling

Wheat straw samples were collected and cut to 100–250 mm in size in the field by harvesters in North Rhine-Westphalia, Germany (August 2016). The collected samples were pressed as straw blocks, with an average mass of 300 kg per block, before storage. Local tap water (ionic concentration Na^+—1.93 mg/L, K^+—0.89 mg/L, Mg^{2+}—2.05 mg/L, Ca^{2+}—8.55 mg/L, Cl^-—4.18 mg/L, $SO_4{}^{2-}$—7.93 mg/L, $NO_3{}^-$—2.57 mg/L) was adopted as a leaching agent in this study. Said et al. [23] reported that tap water made no difference, compared with distilled water, when leaching biomass. Compared with distilled water, tap water has the advantage of being simple, readily available, economical, and feasible. Additionally, tap water is relatively stable and more controllable than natural precipitation [21]. The leaching process began with the main washing process. Each straw block was mixed with tap water, using a solid to liquid ratio of 1:12 (wt./wt.), in a 30 m^3 mixing container (BvL V-Mix2S Plus, Bremen, Germany) with two installed rotors (100 rpm). After 30 min of stirring, the straws and eluate were dumped onto a non-woven geotextile (1.0–1.5 mm) in the field and air dried for 48 h prior to oven drying. The samples were then oven dried (105 °C) in a nearby steam plant. The leaching and drying processes are simple and economical, with an estimated unit cost of €0.22 per kg. For combustion and other analyses, wheat straw samples were chopped using a sequential screening process (i.e., sequentially passed through 5, 2, and 1 mm screens) to ensure that the samples could be completely decomposed during the heating process. Finally, the samples less than 1 mm in particle size were stored in sealed plastic bags in the lab at 20 ± 2 °C.

The wheat straw analyzed in this study is herein referred to as WS_G (the footnote indicating the straw was sampled from Germany), and the wheat straw before and after leaching is referred to as WS_{GO} (original straw) and WS_{GL} (leached straw), respectively.

2.2. Analytical Procedures for Original and Leached Samples

2.2.1. Ash Content, Volatile Matter, and Other Content Tests

The ash content on a dry basis was determined by calculating it from the mass of the residue after heating using the following formula:

$$A_d = \frac{(m_3 - m_1)}{(m_2 - m_1)} \times 100 \times \frac{100}{100 - M_{ad}} \quad (1)$$

where m_1 is the mass of the empty dish, m_2 is the mass of the dish plus the test sample, m_3 is the mass of the dish plus the ash, and M_{ad} is the percentage moisture content of the test sample. The heating process was conducted according to the procedure described in DIN EN ISO 18122. One gram wheat straw specimens were placed in crucibles during the heating process in a muffle oven (Nabertherm LH 30/14, Lilienthal, Germany). The temperature of the muffle oven was uniformly increased to 250 °C at a rate of 7.5 °C/min over a period of 0.5 h. In order that the volatile constituents (such as KCl) could escape from the specimens before combustion, 250 °C was maintained for 1 h. The oven temperature was then uniformly increased to 550 ± 10 °C over a period of 0.5 h at a rate of 10 °C/min, and 550 °C was maintained for 2 h. Following the heating process, the specimens and crucibles were cooled to lab temperature (i.e., 20 °C) on a heat-resistant plate in a desiccator. Ash content generally has a close relation with the melting temperature, and less ash content generates less sinter particles [5,23,27].

For the volatile matter tests, DIN EN ISO 18123 requires the heating of specimens for 7 min at a temperature of 900 ± 10 °C in a muffle oven. After heating, the crucible base was removed from the furnace and cooled to room temperature on a heat-resistant plate in the desiccator. Rapid cooling and storing in the desiccator also minimized the absorption of ambient water by the specimens.

The percentage content of volatile constituents on a dry basis was calculated by subtracting the mass loss of water from the mass loss of the tested sample, as expressed in the following formula:

$$V_d = \frac{(m_3 - m_1)}{(m_2 - m_1)} \times 100 \times \frac{100}{100 - M_{ad}} \quad (2)$$

where m_1 is the mass of the empty dish, m_2 is the mass of the dish plus the test sample, m_3 is the mass of the dish plus the ash, and M_{ad} is the percentage of moisture content of the test sample.

Both original and leached samples were analyzed for moisture and ultimate elemental composition for C, H, N, S, and Cl. The facilities and experimental standards used are presented in Table 1. Moreover, ash-related elements (e.g., Si, K, Mg, Na, Ca, etc.) were tested by an X-ray fluorescence (XRF) test.

Table 1. Facilities and standards for the moisture and ultimate composition tests.

Parameter	Facility	Standard
Moisture	Binder ED056 (Tuttlingen, Germany)	DIN EN 14774
C/H/N	Leco CHN628 (Saint Joseph, USA)	DIN EN 15104
Cl	Schott Titroline Alpha (Mainz, Germany)	DIN 51727
S	Leco SC 144 DR (Saint Joseph, USA)	DIN 51724

2.2.2. Heating Value Test

Heating value tests were conducted in accordance with DIN EN 14918. Half a gram of wheat straw was burnt in a bomb calorimeter (IKA C200, Wilmington, CA, USA) under high pressure oxygen (minimum 40 bar), equipped with an ignition circuit. The higher heating value (HHV) was chosen as an index parameter to evaluate the combustion characteristics of the wheat straw; HHV is widely used as an indicator of the total potential heat in a specimen [18,19,22,28].

2.2.3. Ash Melting Point Test

Hot-stage microscopy (HSM) has been widely used to study the sintering phenomena in biomass ash [4,11,23,24,26,29]. In this study, a side-view hot stage microscope (EM201, Hesse Instruments Company, Osterode am Harz, Germany) was used to determine the sintering phenomena during the ash melting point test, and a schematic image of it is shown in Figure 1. The HSM was equipped with an electrical furnace (Hesse HT-16, Osterode am Harz, Germany) and an image analysis system with a hot stage camera (Leitz CCD camera, Wetzlar, Germany). The HSM software calculates the projection image of the test object in three dimensions (including height, width, and area) to recognize the characteristic temperatures during the melting process.

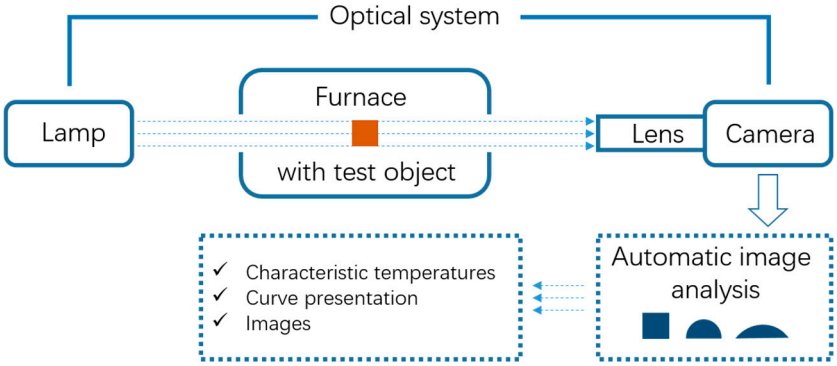

Figure 1. HSM optical system and automatic image analysis.

The image analysis mainly focused on the volume change and morphology of the ash under four key temperatures during melting, which are as follows: (1) shrinkage starting temperature (SST),

(2) deformational temperature (DT), (3) hemispheric temperature (HT), and (4) flow temperature (FT). SST is defined as the temperature at which the area of the projection image of the test object at 550 °C is less than 95%. SST is the temperature indicating that the specimen has started to shrink. DT is often known as the ash fusion temperature, at which the first sign of rounding on the edges of the specimen occurs during the melting process. Because of the frequently occurring shape recognition errors made by computers, the DT is typically manually selected and is also required by DIN CEN/TS 15370-1. HT is the temperature at which the specimen forms an approximate hemisphere. FT is the temperature at which the ash is extended over the support, the height of which is one half the height of the test piece at the hemispheric temperature.

2.2.4. Ash Sintering Degree Test

The ash melting degree test evaluates both by visual inspection and by assessing the microstructure of the specimen. Considering the range of effective temperatures of the lignocellulose biomass by household boilers at a small scale, the ash sintering degree test was conducted at four different temperatures: 700, 800, 900, and 1000 °C. Specimens were placed into a crucible and heated for 2 h in a muffle oven at a selected temperature. After heating, the specimens were removed and placed in desiccators for cooling. All specimens were mounted on aluminum stubs by double-sided adhesive carbon tape. The specimens were then scanned and analyzed using an SEM (Hitachi TM300, Tokyo, Japan) to evaluate the change in microstructure under various heating temperatures.

3. Results and Discussion

3.1. Proximate and Ultimate Analysis

Results of the ultimate elemental composition of the original and leached WS_G are shown in Table 2, where the values represent the weight percentage of dry biomass. To compare the leaching effects on the straws, the leaching data of wheat straw from Yu et al. [25], which are denoted as WS_U, were adopted and compared in Table 2. According to the proximate analysis, the moisture content of WS_{GO} was 6.55%, which is consistent with the dry surrounding environment during storage. A high moisture content of biomass normally wastes more energy during combustion, because the moisture consumes heat for evaporation during the early stage. The volatile matters of WS_{GO} and WS_{UO} were 79.12% and 74.0%. Biomass with a higher content of volatile matter typically has a relatively lower ash content (e.g., the comparison between WS_{GO} and WS_{UO}), and a high content of volatile matter accelerates the combustion process and generates more energy at a given temperature [22]. Therefore, the WS_{GO}, with a slightly higher volatile matter than WS_{UO}, performed better in generating heat. Additionally, the ultimate analysis shows that C was the most dominant element in WS_{GO} (47.62%), while O had the second highest concentration (41.53%). The H, N, S, and Cl contents of WS_{GO} were 6.20, 0.43, 0.06, and 0.02%, respectively, which are similar to WS_U except Cl (H: 5.70%; N: 0.47%; S: 0.11%). Higher Cl contents occurred in WS_{UO} (0.85%), while the Cl content in WS_{GO} was only 0.02%.

The leaching procedure significantly enhanced the C content and volatile matters in the biomass by washing the contaminants attached to the straw surface, e.g., elements brought in during harvesting. A higher C content was found in WS_{GL} (47.83%) compared to that of WS_{GO} (47.62%), which was consistent with the C content in WS_U (which increased from 43.50% to 44.90%) and the results reported by Said et al. [23]. Additionally, the volatile matter slightly increased by 5.32% (from 79.12% in SW_{GO} to 83.33% in SW_{GL}) after leaching. Significant increases in volatile matter were found in WS_{UL}, increasing from 74.00% to 80.30% after leaching. Increases in volatile matter will enhance the energy per unit of dry mass, conveying the benefits of the leaching process [17,26].

Table 2. Results from the tests of original and leached straw samples.

wt.% Dry Biomass	Original (WS_{GO})		Leached (WS_{GL})		Original (WS_{UO}*)	Leached (WS_{UL}*)
	Mean	Standard Deviation	Mean	Standard Deviation		
HHV (MJ/kg)	19.25	0.15	19.53	0.35	17.30	17.25
Volatile Matters	79.12	0.50	83.33	0.37	74.00	80.30
Ash Content	4.14	0.46	3.06	0.50	8.28	6.27
C	47.62	0.43	47.83	0.29	43.50	44.90
H	6.20	0.09	5.99	0.11	5.70	5.70
O	41.53	0.48	42.84	0.28	41.90	42.80
N	0.43	0.03	0.26	0.02	0.47	0.32
S	0.06	0.00	0.02	0.00	0.11	ND
Cl	0.02	0.00	ND	0.00	0.85	NA
Mass of ash-related elements in sample, mg/g dry biomass						
Ca	16.08	1.09	18.64	0.96	1.16	0.94
K	19.18	0.95	7.08	0.40	17.27	3.04
Mg	0.54	0.06	0.38	0.06	1.28	0.60
Na	ND	NA	ND	NA	1.92	0.80
Si	16.64	3.21	15.93	1.89	17.90	23.18

*: data came from Yu et al. [25]; ND: not detected; NA: not available.

Both WS_{GO} and WS_{GL} showed a relatively low ash content, at 4.14% and 3.06%, respectively. The ash removal efficiency after leaching was 26.09%, which is largely due to the removal of a great number of ash particles, as well as some alkaline metals (such as K) and partial Cl and S contents in the biomass [24,30]. WS_{UO} showed relatively higher ash contents (8.28%) compared to WS_{UL} (6.27%) after washing. Generally, the ash content is inversely related to the biomass combustion efficiency. High ash content in biomass decreases the heating value and generates ash-related problems, e.g., precipitation on the inner surface of the boiler, when applying biomass as a solid fuel [22]. A significant removal of Cl, S, and N occurred after leaching with water. Cl was completely washed away, with non-detectable Cl content in WS_{GL} after leaching. The Cl content was also non-detectable in WS_{UL}. Similar to Cl, S is often regarded as a diffluent element (occurring as sulfate). The S content decreased by 66.67% (from 0.06% to 0.02%) in WS_G after leaching, while the S removal of WS_U was nearly 100%.

Differences between the proximate analysis and ultimate analysis can be recognized, although the leaching process has similar effects—of increasing (C and volatile matters) and decreasing (ash, Cl, S, and N) compounds in both WS_G and WS_U.

3.2. Removal of Ash-Related Elements in Samples

The major ash-related elements detected in the biomass samples were Ca, K, Mg, Na, and Si (Table 2). In WS_{GO}, the Ca, K, Mg, and Si contents were 16.08, 19.18, 0.54, and 16.64 mg/g, respectively. Generally, the leaching process showed a high efficiency in the removal of ash-related elements, and similar results were found in other studies [17,31,32]. WS_{GL} showed a significant decrease in K (7.08 mg/g) and Mg (0.38 mg/g) contents after leaching, and the removal ratios were 63.1% and 29.6%, respectively. Additionally, the Si in WS_{GL} slightly decreased to 15.93 mg/g (16.64 mg/g in WS_{GO}), at a reduction ratio of 4.3%. Si is the major element of clays, as clay minerals are the major silicates [3]. The washing of ash particles, including clays, attached to the straw surface may be the reason for the reduction of Si. However, the Ca content in WS_G increased by 15.9% (from 16.0 to 18.64 mg/g), while WS_U showed a reduction in Ca after leaching. Additionally, the Ca in WS_G was 14.5 times higher than in WS_U, which is likely due to the variation in biomass types or cultivation ambience (e.g., water hardness and soil condition).

3.3. HHV

The HHV of the WS_{GO} reached 19.25 MJ/kg, with a standard deviation of 0.15 from the triplicate tests. The HHV of WS_{GL} slightly increased by 1.45% (19.53 MJ/kg) after leaching. Chin et al. [22] reported an inversely linear relationship between ash content and HHV. Similar results were also found by Jenkins et al. [16] and Obernberger et al. [33]. The biomass HHV is considered to be strongly related to organic compounds [25]. The ash content reduction results in a relatively higher content of organic matter (e.g., lignocellulose and volatile matter), consequently increasing the HHV. The biomass heating value represents the calorific release while burning in the furnace. Improving HHV obviously enhances the energy potential of wheat straw as a biomass solid fuel.

3.4. Ash Melting Test

Results of the ash melting test are shown in Figure 2. Generally, the combustion temperature of household boilers at a small scale ranges from 1000 to 1200 °C (the orange color marked in Figure 2). The shrinkage of ash in WS_{GO} began at 700 °C (SST), while round angles in the ash were first evident at approximately 910 °C (DT). The FT of the WS_{GO} was found at 1130 °C. Therefore, in the temperature range of household boilers at a small scale (1000–1200 °C, marked in Figure 2), WS_{GO} is easily fused and transformed from solid to liquid. Similar results were also reported by Ma et al. [34] and Niu et al. [11]. The results show that the original wheat straw collected in this study was significantly melted during combustion. A similar melting phenomenon is also likely to occur when using WS_{UO}, because the SST and DT are relatively lower than the minimum temperature of the boiler (1000 °C). The SST of WS_{UO} (800 °C) was 100 °C higher than that of WS_{GO} (700 °C), while the differences in the DT were negligible.

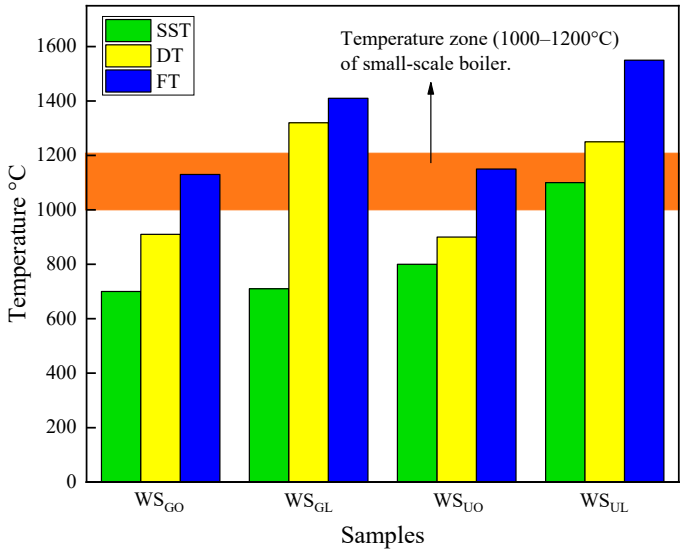

Figure 2. Melting temperatures of original and leached samples. The results concerning WS_{UO} and WS_{UL} were obtained from Yu et al. [25], for comparison.

The leaching process effectively improved the ash melting temperatures. Generally, biomass fuels with high ash melting temperatures (beyond the boiler temperature) generate less sinters while burning. The SST of WS_{GL} was 10 °C higher than that of WS_{GO} after leaching. However, a more drastic increase in DT and FT was observed after leaching. The DT and FT of WS_{G} increased by 410 °C (from 910 to 1320 °C) and 280 °C (from 1130 to 1410 °C) respectively, indicating that leaching by water greatly impacts the deformational behavior of ashes. Both the DT and FT are beyond the combustion temperature zone of small-scale household boilers, indicating that ash melting is unlikely to occur during combustion. Jenkins et al. [20] and Bakker et al. [21] found that the removal of ashes and absorption K via leaching could evidently improve the melting temperature, which is

consistent with WS_U. Additionally, leaching can decrease the opportunities for a K-silicate (e.g., mica), which is considered a byproduct at a low melting temperature and theoretically promotes the sintering temperature [35], to be formed.

3.5. Sintering Degree Test

To observe ash sintering behavior at different temperatures, the ash sintering degrees at selected temperatures (i.e., 700, 800, 900, and 1000 °C) were evaluated. Incremental temperatures were chosen for the ash sintering degree test, considering operational experience, which tells us that crop biomass burns in boilers within a certain temperature range. Both the original and leached samples were then heated in a muffle oven under the aforementioned temperatures.

Macroscopic and microscopic images of WS_{GO} and WS_{GL} ashes heated at 700–1000 °C are shown in Figures 3 and 4, respectively. Only a slight amount of WS_{GO} ash remained after heating at 1000 °C. The melted ash strongly adhered to the crucible and formed hard and dense sediment, which was difficult to segregate and photograph under SEM (Figure 3d). Therefore, no SEM image of the macrostructure of WS_{GO} is provided in this study. No severe sintering was found from the heated ashes in the crucible at 700 °C, and the WS_{GO} ash was easily ground to powder. The SEM analysis shows that the molten structure of WS_{GO} was evident at 700 °C. However, a loosely packed structure (a porous structure) is dominant at 20 micron magnification (Figure 3a). The molten structure was observed to have a dark and smooth surface, and is considered to be an intuitionistic sintering part (point 2 on Figure 3a). Unmelted compounds are represented in a light gray color and are of a loose ash condition (point 1 on Figure 3a). Severe sintering appeared when the ash was heated to temperatures higher than 800 °C. At 800 °C, ash diffusion occurred in the crucible. Some of the ash particles were consolidated into a solid structure. The molten structure with a dark surface (point 4 on Figure 3b) formed larger grains than that at 700 °C, with loosely packed ash attached to the surface (point 3 on Figure 3b). Strong sintering was observed when the structure was heated to 900 °C, though no sign of wheat straw ash debris was found in the crucible (Figure 3c). Additionally, the loosely packed ashes observed at lower temperatures (<900 °C) completely melted at 900 °C (point 5 on Figure 3c).

The ash after leaching showed similar macro and microstructures as that of the original ash at 700 °C (Figure 4a). However, wheat straw ashes after leaching showed an obvious porous structure in the SEM images at 800 °C (Figure 4b). Loose ashes (Point 6 on Figure 4a and Point 8 on Figure 4b) adhered to the molten areas (Point 7 on Figure 4a and Point 9 on Figure 4b). Ash heated to 800 °C showed an incompact appearance, although the microstructure was evident in the porous condition, indicating that the washed wheat straw ash was slightly melted and classified as slightly sintered. Sintering appeared as the heating temperature increased to 900 °C (Figure 4c). Unmolten ashes (Point 10 in Figure 4c) still existed at 900 °C, indicating that WS_{GL} performed better than WS_{GO} at 900 °C, which revealed that wheat straw after leaching had a negative tendency to generate sinters under this condition. An SEM image of WS_{GL} ash heated at 1000 °C is shown in Figure 3d. The ashes were primarily pale in color, with a small amount of ash forming a hard and dense precipitate, which was different than that of WS_{GO}. Un-sintered particles (Point 11 in Figure 4d) with a similar microstructure to that of Point 5 in Figure 4c were observed under SEM. Melted particles existed in WS_{GL}, although, unlike in WS_{GO}, the leaching process had already decreased the risk of sintering at 1000 °C.

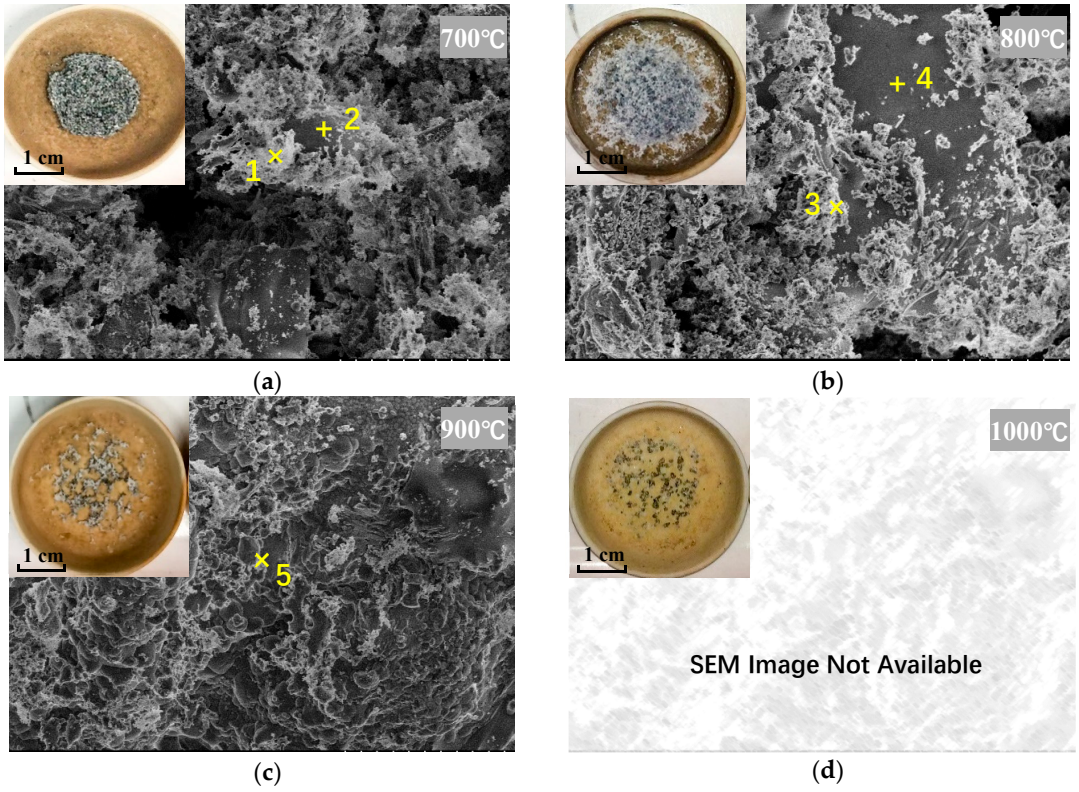

Figure 3. SEM images of WS_{GO} ashes: (**a**) WS_{GO} ash heated to 700 °C, (**b**) WS_{GO} ash heated to 800 °C, (**c**) WS_{GO} ash heated to 900 °C, and (**d**) WS_{GO} ash heated to 1000 °C (SEM image was not available).

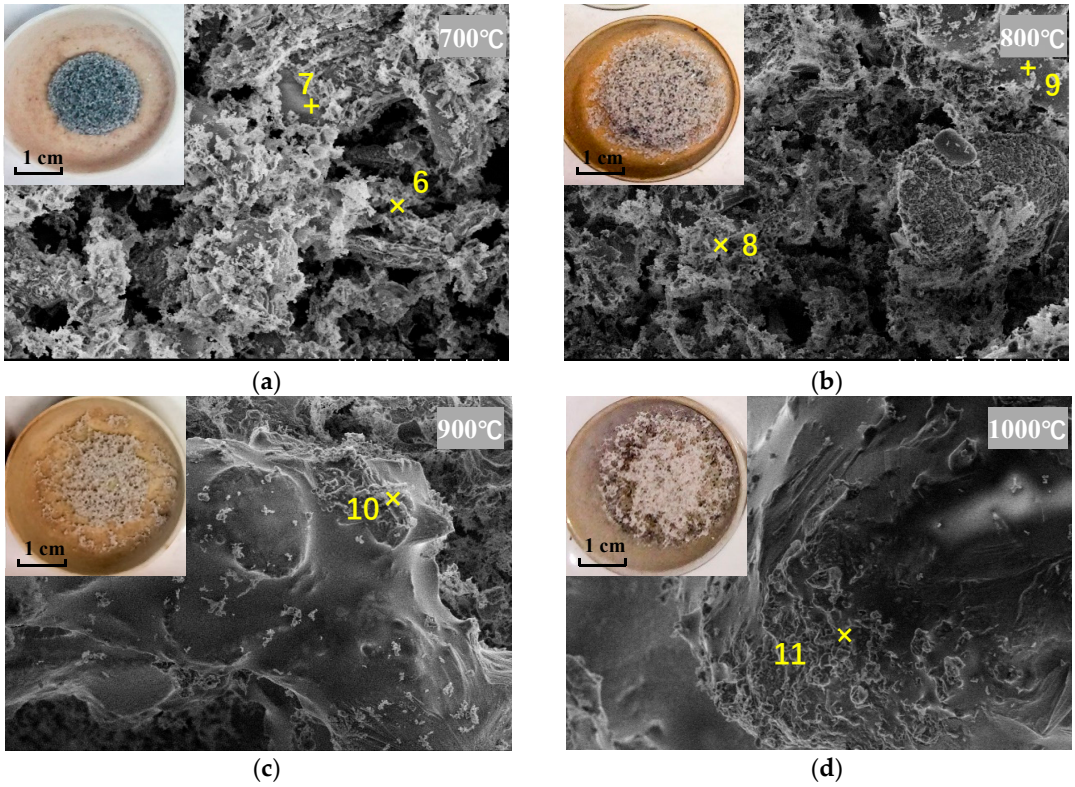

Figure 4. SEM images of WS_{GL} ashes: (**a**) WS_{GL} ash heated to 700 °C, (**b**) WS_{GL} ash heated to 800 °C, (**c**) WS_{GL} ash heated to 900 °C, and (**d**) WS_{GL} ash heated to 1000 °C.

Wang et al. [5,27] classified biomass ashes into five sintering degrees based upon the microstructure, which are as follows: (1) loose ash without aggregates and slag formation; (2) slightly sintered ash, with an easily broken fragile structure; (3) hard, sintered ash with partial melting; (4) very hard, sintered ash, related to formation of heavy sinters and slag; and (5) completely melted.

The sintering degrees of leached and unleached biomass used in this study at different temperatures are shown in Figure 5. At 700 °C, WS_{GO} and WS_{GL} were both slightly sintered and classified as Degree 2. However, WS_{GO} showed more severe sintering after 700 °C. WS_{GO} samples heated at 800, 900, and 1000 °C were hard sintered (Degree 3), very hard sintered (Degree 4), and completely melted (Degree 5), respectively. The sintering degree of WS_{GL} was generally lower than that of WS_{GO}, indicating that leaching improved the wheat straw sintering characteristics. The sintering degrees of WS_{GL} increased from slight sintering (Degree 2) to very hard sintering (Degree 4) from 800 °C to 1000 °C. The effectiveness of leaching is generally attested to, e.g., by Said et al. [23].

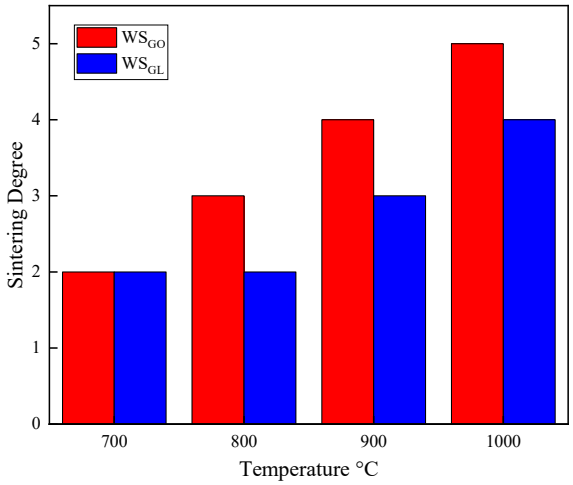

Figure 5. Sintering degrees of original and leached samples at different temperatures. (Degrees: 1: loose ash, 2: slightly sintered, 3: hard sintered, 4: very hard sintered, 5: completely melted).

3.6. Predicting Model of Ash Sintering by Ash-Related Elements

The results of the partial correlation analysis of biomasses from the literature and current study are shown in Table 3. The analysis aims to investigate the partial correlation between ash-related elements (Si, Mg, Ca, Na, and K) and SST, which is considered to be the temperature when biomass ash starts to sinter [11]. A higher SST is preferable for combustion, because there is less chance of agglomeration. By conducting partial correlation analysis, the variance in a particular variable is partitioned into components attributable to different sources of variation, and the statistical significance of each variable on the variance can be clarified.

Table 3. Selected biomass data of ash-related elements and shrinkage starting temperature (SST).

Biomass	Mass of Ash-Related Elements in Ash (wt.%)					SST (°C)	Source
	Si	Mg	Ca	Na	K		
Pine	24.27	2.7	9.29	1.41	6.56	1190	[36]
Eucalyptus	19.13	2.52	12.86	1.41	7.22	1160	[36]
Poplar	1.31	2.22	23.57	0.1	14.94	1400	[36]
Wheat straw	20.53	1.44	5.79	0.16	14.94	850	[36]
Rice straw	23.8	2.1	6.36	2.08	13.28	860	[36]
Barley husk	14.83	0.03	5.44	0	23.04	856	[27]
Barley straw	12.83	1.75	13.88	0.28	27.91	960	[27]
Wood	10.5	3.34	19.92	0.22	5.58	1160	[37]
Wood	10.37	3.64	30.74	2.11	8.92	1192	[38]
Herbaceous	15.58	3.37	10.61	1.7	22.11	979	[38]
Grasses	21.55	2.41	8.02	0.93	20.4	970	[38]
Straw	20.51	2.8	10.09	1	20.32	857	[38]
Pine sawdust	10.75	4.97	31.01	1.21	7.68	1194	[39]
Corn stalk	12.14	7.21	5.68	1.77	29.8	1001	[39]
Corn straw	11.82	2.96	6.86	0	28.01	960	[34]
Rice straw	18.04	3.31	5.78	1.01	21.53	890	[34]
Wheat straw	19.2	1.12	4.91	0.22	20.51	890	[34]
Peanut shell	10.35	4.75	15.27	0.93	19.62	1130	[34]
Rice husk	29.65	2.75	1.46	0.19	8.86	1140	[34]
Sawdust	15.51	1.21	26.76	1.53	3.8	1240	[34]
WS_{GO}	16.64	0.54	16.08	0	19.18	700	
WS_{GL}	15.93	0.38	18.64	0	7.08	800	

The results of partial correlation analysis are shown in Table 4. K (–0.617) had the most significant negative effects on SST (p-value: 0.011 < 0.05) among all five elements. Si (–0.366) and Mg (+0.351) are possibly related to SST, although the p-values were higher than 0.05. Na (–0.162) showed no evident correlation to SST, whereas Ca (+0.005) showed no correlation (p-value: 0.985; >0.95). Therefore, the concentration of K is the main factor affecting the ash sintering temperature. Positive effects of Ca and Mg on ash sintering problems have been proven to buffer the negative impact of K; as a result, the K/(Ca + Mg) ratio is proposed to indicate the ash sintering tendency [26,36,40]. Tonn et al. [26] noted that grassland biomass with a K/(Ca + Mg) ratio of 0.23 had a strong chance of being loose ash, whereas it was easily sintered when the K/(Ca + Mg) ratio was as high as 1.75, indicating that the high K/(Ca + Mg) ratio more likely causes ash sintering. In this study, the K/(Ca + Mg) ratio of wheat straw (i.e., WS_G) decreased from 1.15 to 0.37 after leaching, evidently improving the ash sintering characteristics via the leaching process.

Table 4. Partial correlation analysis results.

SST	Si	Mg	Ca	Na	K
Correlation	−0.366	+0.351	+0.005	−0.162	−0.617
p-value	0.164	0.183	0.985	0.550	0.011

+/−: positive/negative value.

4. Conclusions

The leaching of ash from biomass using water could be an economical and feasible technique to prevent ash-related problems. In this study, the ash in wheat straw was washed using tap water, and the ash content decreased by 26.09% (from 4.14 to 3.06%). The leaching process had effects on compounds, increasing C and volatile matters and decreasing ash, Cl, S, and N of the wheat straw. Moreover, K showed the highest removal rate compared to that of other elements after leaching,

including Ca, Mg, Cl, and S. The leaching process also enhanced the C content and volatile matters, which resulted in the increase of HHV.

The leaching process effectively improved the ash melting temperatures in DT and FT. The microstructural images from SEM of WS_{GO} and WS_{GL} obviously showed more melted parts in WS_{GO} than in WS_{GL} at the same temperature, and the sintering degrees of WS_{GL} were lighter than those of WS_{GO}, which indicates that leaching remits the ash sintering problem. K is the main cause of the lower ash sintering temperature, which must be significantly decreased by partial correlation analysis. The K/(Ca + Mg) ratio decreased considerably, which evidently showed the removal of K in the wheat straw. Consequently, the leaching of K from wheat straw was proven to have positive effects on the ash sintering problem.

Author Contributions: Conceptualization, S.W. and J.C.; methodology, S.W.; software, S.W.; validation, J.C., and D.P.; formal analysis, S.W.; investigation, S.W.; resources, J.C. and D.P.; data curation, S.W.; writing—original draft preparation, S.W., Z.W. and Q.L.; writing—review and editing, S.W. and J.C.; visualization, J.C.; supervision, J.C.; funding acquisition, D.P. and T.H.

Funding: This research was funded by China Fundamental Research Funds for the Central Universities, grant number 2682016CX095, and Sichuan Provincial Key Technology Support, grant number 2016HH0084.

Acknowledgments: This research was supported by the Unit of Technologies of Fuels of RWTH-Aachen University and China Scholarship Council Program. The experiments were directed by Peter Georg Quicker, Thomas Horst, Lukas Schenke, Yves Noel and Georg Grünheidt.

Conflicts of Interest: The authors declare no conflict of interest. The funders had no role in the design of the study, in the collection, analyses, or interpretation of data, in the writing of the manuscript, or in the decision to publish the results.

References

1. International Energy Agency (IEA). World Energy Outlook. Available online: http://www.iea.org/publications/freepublications/publication/world-energy-outlook-2012.html (accessed on 8 March 2018).
2. Facts about Climate Change, Conserve Energy Future. Available online: https://www.conserve-energy-future.com/various-climate-change-facts-php.php (accessed on 8 March 2018).
3. Boström, D.; Skoglund, N.; Grimm, A.; Boman, C.; Öhman, M.; Broström, M.; Backman, R. Ash transformation chemistry during combustion of biomass. *Energy Fuels* **2012**, *26*, 85–93. [CrossRef]
4. Ghaly, A.E.; Al-Taweel, A. Physical and thermochemical properties of cereal straws. *Energy Sources* **1990**, *12*, 131–145. [CrossRef]
5. Wang, L.; Skjevrak, G.; Hustad, J.E.; Skreiberg, Ø. Investigation of biomass ash sintering characteristics and the effect of additives. *Energy Fuels* **2014**, *28*, 208–218. [CrossRef]
6. Werther, J.; Saenger, M.; Hartge, E.; Ogada, T.; Siagi, Z. Combustion of agricultural residues. *Prog. Energy Combust. Sci.* **2000**, *41*, 1–27. [CrossRef]
7. Nunes, L.J.R.; Matias, J.C.O.; Catalão, J.P.S. Mixed biomass pellets for thermal energy production: A review of combustion models. *Appl. Energy* **2014**, *127*, 135–140. [CrossRef]
8. Emil, D. Co-firing biomass with coal for power generation. In Proceedings of the Intensive Programme 2014, Pardubice, Czech Republic, 6–17 July 2014.
9. Li, L.; Yu, C.; Huang, F.; Bai, J.; Fang, M.; Luo, Z. Study on the deposits derived from a biomass circulating fluidized-bed boiler. *Energy Fuels* **2012**, *26*, 6008–6014. [CrossRef]
10. Niu, Y.; Du, W.; Tan, H.; Xu, W.; Liu, Y.; Xiong, Y.; Hui, S. Further study on biomass ash characteristics at elevated ashing temperatures: The evolution of K, Cl, S and the ash fusion characteristics. *Bioresour. Technol.* **2013**, *129*, 642–645. [CrossRef]
11. Niu, Y.; Tan, H.; Wang, X.; Liu, Z.; Liu, H.; Liu, Y.; Xu, T. Study on fusion characteristics of biomass ash. *Bioresour. Technol.* **2010**, *101*, 9373–9381. [CrossRef]
12. Nielsen, H.P.; Frandsen, F.J.; Dam-Johansen, K.; Baxter, L.L. The implications of chlorine-associated corrosion on the operation of biomass-fired boilers. *Prog. Energy Combust. Sci.* **2000**, *26*, 283–298. [CrossRef]
13. Liu, H.; Feng, Y.; Wu, S.; Liu, D. The role of ash particles in the bed agglomeration during the fluidized bed combustion of rice straw. *Bioresour. Technol.* **2009**, *100*, 6505–6513. [CrossRef]

14. Lindberg, D.; Backman, R.; Chartrand, P.; Hupa, M. Towards a comprehensive thermodynamic database for ash-forming elements in biomass and waste combustion—Current situation and future developments. *Fuel Process. Technol.* **2013**, *105*, 129–141. [CrossRef]
15. Kassman, H.; Pettersson, J.; Steenari, B.M.; Åmand, L.E. Two strategies to reduce gaseous KCl and chlorine in deposits during biomass combustion—Injection of ammonium sulphate and co-combustion with peat. *Fuel Process. Technol.* **2013**, *105*, 170–180. [CrossRef]
16. Jenkins, B.M.; Baxter, L.L.; Miles, T.R.; Miles, T.R. Combustion properties of biomass. *Fuel Process. Technol.* **1998**, *54*, 17–46. [CrossRef]
17. Liaw, S.B.; Wu, H. Leaching characteristics of organic and inorganic matter from biomass by water: Differences between batch and semi-continuous operations. *Ind. Eng. Chem. Res.* **2013**, *52*, 4280–4289. [CrossRef]
18. Yu, C.; Zheng, Y.; Cheng, Y.S.; Jenkins, B.M.; Zhang, R.; VanderGheynst, J.S. Solid-liquid extraction of alkali metals and organic compounds by leaching of food industry residues. *Bioresour. Technol.* **2010**, *101*, 4331–4336. [CrossRef] [PubMed]
19. Turn, S.Q.; Kinoshita, C.M.; Ishimura, D.M. Removal of inorganic constituents of biomass feedstocks by mechanical dewatering and leaching. *Biomass Bioenerg.* **1997**, *12*, 241–252. [CrossRef]
20. Jenkins, B.M.; Mannapperuma, J.D.; Bakker, R.R. Biomass leachate treatment by reverse osmosis. *Fuel Process. Technol.* **2003**, *81*, 223–246. [CrossRef]
21. Bakker, R.R.; Jenkins, B.M. Feasibility of collecting naturally leached rice straw for thermal conversion. *Biomass Bioenerg.* **2003**, *25*, 597–614. [CrossRef]
22. Chin, K.L.; H'ng, P.S.; Paridah, M.T.; Szymona, K.; Maminski, M.; Lee, S.H.; Lum, W.C.; Nurliyana, M.Y.; Chow, M.J.; Go, W.Z. Reducing ash related operation problems of fast growing timber species and oil palm biomass for combustion applications using leaching techniques. *Energy* **2015**, *90*, 622–630. [CrossRef]
23. Said, N.; Bishara, T.; García-Maraver, A.; Zamorano, M. Effect of water washing on the thermal behavior of rice straw. *Waste Manag.* **2013**, *33*, 2250–2256. [CrossRef]
24. Deng, L.; Zhang, T.; Che, D. Effect of water washing on fuel properties, pyrolysis and combustion characteristics, and ash fusibility of biomass. *Fuel Process. Technol.* **2013**, *106*, 712–720. [CrossRef]
25. Yu, C.; Thy, P.; Wang, L.; Anderson, S.N.; Vandergheynst, J.S.; Upadhyaya, S.K.; Jenkins, B.M. Influence of leaching pretreatment on fuel properties of biomass. *Fuel Process. Technol.* **2014**, *128*, 43–53. [CrossRef]
26. Tonn, B.; Thumm, U.; Lewandowski, I.; Claupein, W. Leaching of biomass from semi-natural grasslands—Effects on chemical composition and ash high-temperature behaviour. *Biomass Bioenerg.* **2012**, *36*, 390–403. [CrossRef]
27. Wang, L.; Becidan, M.; Skreiberg, Ø. Sintering behavior of agricultural residues ashes and effects of additives. *Energy Fuels* **2012**, *26*, 5917–5929. [CrossRef]
28. Pronobis, M.; Wojnar, W. The impact of biomass co-combustion on the erosion of boiler convection surfaces. *Energy Convers. Manag.* **2013**, *74*, 462–470. [CrossRef]
29. Pintana, P.; Tippayawong, N. Predicting ash deposit tendency in thermal utilization of biomass. *Eng. J.* **2016**, *20*, 15–24. [CrossRef]
30. Liu, X.; Bi, X.T. Removal of inorganic constituents from pine barks and switchgrass. *Fuel Process. Technol.* **2011**, *92*, 1273–1279. [CrossRef]
31. Ogden, C.A.; Ileleji, K.E.; Johnson, K.D.; Wang, Q. In-field direct combustion fuel property changes of switchgrass harvested from summer to fall. *Fuel Process. Technol.* **2010**, *91*, 266–271. [CrossRef]
32. Vamvuka, D.; Zografos, D.; Alevizos, G. Control methods for mitigating biomass ash-related problems in fluidized beds. *Bioresour. Technol.* **2008**, *99*, 3534–3544. [CrossRef]
33. Obernberger, I.; Thek, G. Physical characterisation and chemical composition of densified biomass fuels with regard to their combustion behaviour. *Biomass Bioenerg.* **2004**, *27*, 653–669. [CrossRef]
34. Ma, T.; Fan, C.; Hao, L.; Li, S.; Song, W.; Lin, W. Fusion characterization of biomass ash. *Thermochim. Acta* **2016**, *638*, 1–9. [CrossRef]
35. Steenari, B.M.; Lundberg, A.; Pettersson, H.; Wilewska-Bien, M.; Andersson, D. Investigation of ash sintering during combustion of agricultural residues and the effect of additives. *Energy Fuels* **2009**, *23*, 5655–5662. [CrossRef]
36. Llorente, M.J.F.; García, J.E.C. Comparing methods for predicting the sintering of biomass ash in combustion. *Fuel* **2005**, *84*, 1893–1900. [CrossRef]

37. Reinmoeller, M.; Klinger, M.K.; Thieme, E.; Meyer, B. Analysis and prediction of slag-induced corrosion of chromium oxide-free refractory materials during fusion of coal and biomass ash under simulated gasification conditions. *Fuel Process. Technol.* **2016**, *149*, 218–230. [CrossRef]
38. Vassilev, S.V.; Baxter, D.; Vassileva, C.G. An overview of the behaviour of biomass during combustion: Part II. Ash fusion and ash formation mechanisms of biomass types. *Fuel* **2014**, *117*, 152–183. [CrossRef]
39. Xiong, Q.; Li, J.; Guo, S.; Li, G.; Zhao, J.; Fang, Y. Ash fusion characteristics during co-gasification of biomass and petroleum coke. *Bioresour. Technol.* **2018**, *257*, 1–6. [CrossRef] [PubMed]
40. Paulrud, S.; Nilsson, C.; Oehman, M. Reed canary-grass ash composition and its melting behavior during combustion. *Fuel* **2001**, *80*, 1391–1398. [CrossRef]